THEORYTICAL STUDY OF PHYSICAL PROPERTIES OF Co_2VZ (Z= Si, Ge) AND CoVZ (Z= Si, Ge) COMPOUNDS USING FIRST PRINCIPLE METHOD

Pardeep Kumar Jangra[1,2], Sitender Singh[1], Sukhender[3]

Article History: Received: 28.08.2023 Revised: 11.09.2023 Accepted: 29.09.2023

Abstract:
Using first principles approaches, the structural, electrical, elastic, and magnetic characteristics of $L2_1$ structured Co_2VZ (Z= Si, Ge) complete Heusler alloys with space group Fm-3m and half-Heusler CoVZ (Z= Si, Ge) compounds with space group F-43_m were examined. The full potential linearized augmented plane wave (FP-LAPW) approach, as implemented in WIEN2k, is used here. Co_2VSi exhibits zero band gaps in both the majority and minority spin channels, whereas Co_2VGe exhibits a finite band gap of 0.668 eV in the minority spin channel and zero band gaps in the majority spin channel around the Fermi level implemented in the WIEN2k code, exhibiting 100% spin polarization. As a result, Co_2VGe is discovered to be perfectly half-metallic ferromagnetic (HMF), whereas Co_2VSi is metallic in nature. In both spin channels, CoVZ (Z= Si, Ge) compounds exhibit semiconducting behavior. Co_2VZ (Z= Si, Ge) compounds have computed magnetic moments of 3.04 and 3.01 B, respectively, whereas CoVZ (Z= Si, Ge) compounds have zero magnetic moment. Here, we see that the code's and Slater-Pauling rule's estimated results have good tuning. Pugh's ratio B/G values are more than 1.75 for all ductile compounds except CoVGe, which is brittle in nature. Because a positive value of Cauchy pressure ($CP = C_{12} - C_{44}$) indicates ductile nature and a negative value indicates brittle nature, we can conclude that all compounds are ductile except CoVGe, which is brittle. Pugh's ratio and Cauchy pressure both produce similar results.

KEYWORDS: Half-metallic ferromagnetic, Semiconducting, Band gap, Spintronics, Magnetic moment

[1]Department of Chemistry, Baba Matnath University, Astal Bohar, Rohtak,(India)
[2]Department of Chemistry, G. C. W., Badhra (India)
[3]Department of Physics, GDC Memorial College Behal (India)

***Corresponding Author:** Pardeep Kumar Jangra
[*]Department of Chemistry, Baba Matnath University, Astal Bohar, Rohtak,(India), pkjchem@gmail.com

DOI: 10.53555/ecb/2023.12.Si13.227

INTRODUCTION:

Numerous analysts and researchers have demonstrated in their research on the investigation of clever and multi-utilitarian materials that may be used for various purposes such as sensors, optoelectronics, spintronics, thermoelectric, and other environmentally friendly power applications. We are looking for materials that can be used as photovoltaics and thermoelectric generators. By using photovoltaics, a massive amount of sunlight-based energy may be consumed and converted into valuable electrical energy, whereas the utilization of distributed heat with thermoelectric generators can gain improved energy maintainability [1-6]. This idea also addresses the need for environmentally sustainable power energy resources. Many materials have been used as potential photovoltaic and thermoelectric devices, including chalcogenides, cross breed perovskites, oxide perovskites, natural mixes, skutterudites, triple point metals, and Half-Heuslers [7-14]. Many researchers have been drawn to half-Heusler materials because of their wide range of applications, simple glasslike structure, and captivating properties such as high liquefying point, attraction, half metallicity, piezoelectric semiconductors, optoelectronic, topological protectors, semimetals, and thermoelectricity [15-25]. Aside from potential thermoelectric applications, Half-Heusler can also be used as a potential candidate for superconductors, spintronics, heat transfer, the production of high-temperature acoustical devices, and protection for strong radiation, photovoltaic application, and laser diodes [26-32]. Heusler materials appeared following Fredrich Heusler's discovery of Heusler amalgams in 1903 [33]. Half Heusler and Full Heusler are the two major types of Heusler materials. Half Heusler materials are F-43m space bunch materials that can be classified into two types based on their VEC. VEC 8 is present in some materials, while VEC 18 is present in others. The whole Heusler compound has a space group of (225) Fm-3m. Because of its unique approach in Spintronics [34-35], the half metallic ferromagnetic behavior of Heusler alloys intrigues new researchers. If one spin channel has a band gap and the other has a zero band gap at the Fermi level, the Heusler compounds have 100% spin polarisation [36-40]. De Groot discovered half metallic ferromagnetic in the year 1983 in a half Heusler compound NiMnSb [41-43]. Heusler has piqued the curiosity of researchers due to its high Curie temperature and spin magnetic moment. Zerrouki et al. [44] investigated various actual boundaries of NbCoSn and NbFeSb half-Heusler materials and concluded that they are precisely stable, flexibly anisotropic, and vulnerable to versatile disfigurement, and that these materials can act as promising thermoelectric and photovoltaic competitors. Asfour [45] investigated the characteristics of Cr2Ta-Ge1-xSnx quaternary Heusler compounds in various x configurations. These varieties of configurations have been seen to be perfectly stable and to exhibit half-metallic behavior, and are likely to be a candidate for optoelectronic applications. Mostari et al. [46] calculated several actual properties of RuVAs under tension and discovered that this material gets temperamental when strain is increased by more than 40 GPa. Similarly, the metallicity of these materials increases with increasing pressure, and at 40 GPa, it enters complete stage advancement. Javed et al. [47] investigated the mechanical dependability and electronic structure of CrVZ (Z S, Se, and Te) and discovered that they are exactly and vibrationally stable against variable deformities. These magnetically stable materials can be seen as a promising candidate for spintronics applications. We will use the WIEN2k code within the Generalized-gradient approximation (GGA) for exchange correlation functions to examine the properties of Co-based full Heusler compounds Co2VZ (Z= Si, Ge) and Half Heusler compounds CoVZ (Z= Si, Ge).

COMPUTATION DETAILS:

Full-potential linearized augmented plane wave (FP-LAPW) [48] approach implemented in Wien2k code [49] was used to calculate the physical fundamental parameters of full Heusler alloys and half Heusler compounds. We select a reasonable Perdew, Burke, and Ernzerhof (PBE) approximation [50-51] for regulating the exchange and correlation potential energy. Generalized-gradient approximation (GGA) [52] was utilized to optimize parameters such as RK_{max}, K-Point, lattice constant, and optimized energy. The exchange-correlation function was authorized. All computations were performed with the spin orbit coupling effect in mind. WIEN2k solids code accurately does electronic structure calculations. The energy between these two states (cut off parameter) was adjusted to -6.0Ry when core states are considered relativistically and valence states are considered semi-relativistically. This code has 1000 k-points in the first Brillouin zone. However, we must specify the number of k-points to be employed in the computation of optical characteristics, and the new value of k-points is 10000. The size of the basis sets is determined by the convergence or cutoff parameter, which has the value R_{mt} K_{max} set to 7.0. The lowest radius of a muffin-tin sphere in a plane wave is denoted by

R_{mt}, while the maximum modulus for a reciprocal lattice vector employed in the elaboration of a flat wave function is given by K_{max}. 0.0001Ry was chosen as the energy convergence criterion. The value of angular momentum maximum (l_{max}) is selected as 10 to enlarge the spherical harmonics in the atomic sphere. The charge density and potential in the centre region were developed as a cheerier series with wave vectors up to G_{max}=10.

RESULTS AND DISCUSSIONS:

Structural Study: The whole Heusler compound has a space group of (225) Fm-3m. The chemical formula for complete Heusler is X_2YZ (X = Co, Y = V, and Z = Si, Ge) with an L21 structure, indicating a 2:1:1 composition. Three penetrating FCC-lattices with atomic locations at X1 (1/4, 1/4, 1/4), X2 (3/4, 3/4, 3/4), Y (1/2, 1/2, 1/2), and Z (0, 0, 0) compose its structure. Where the atoms X and Y are transition metals and the atom Z is a main group metal or semimetal [53-54]. Half-Heusler compounds crystallize in the face-centered cubic structure with the structural classification C1b and the space group F-43_m. These compounds are V with Co, Mn with Ru, Fe, Ni, and Pd produce zinc blend sublattic organized in a primitive cell at Wyckoff positions (0, 0, 0) and (1/4, 1/4, 1/4), whereas NaCl sublattice is formed by V and Z in CoVZ compounds, and Y and Z in MnXY compounds at (1/2, 1/2, 1/2). The equation of state given by Murnaghan [55] gives the value of total energy & pressure as a function of volume is stated as:

$$E(V) = E_O + \left[\frac{BV}{B_P}\left(\frac{1}{(B_P-1)}\left(\frac{V_O}{V}\right)^{B_P} + 1\right) - \frac{BV_O}{(B_P-1)}\right]$$

$$P(V) = \frac{B}{B_P}\left\{\left(\frac{V_O}{V}\right)^{B_P} - 1\right\}$$

Where, Pressure $(P) = -\frac{dE}{dV}$, $B_P = -V\frac{dP}{dV} = V\frac{d^2E}{dV^2}$

E0 is the minimal energy at T = 0K, B is the bulk modulus, BP is the pressure derivative of the bulk modulus, and V_o is the equilibrium volume in the preceding equations. Figure 1 depicts the results of the operation volume optimization for stable structure. In compared to the others, the compound Co2VGe has the highest value of bulk modulus. Table 1 shows the calculated values of the optimized lattice parameter, equilibrium energy, and pressure derivative.

Table 1: Lattice Parameter, Bulk modulus, Equilibrium energy and Pressure derivative for Co_2VZ (Z= Si, Ge) and CoVZ (Z= Si, Ge)

Compound	Lattice Constants a_0 (Å)	Bulk modulus (GPa)	Equilibrium Energy (Ry)	Pressure derivative (GPa)
Co_2VSi	5.685	234.369	-8052.753	5.406
Co_2VGe	5.776	266.241	-11670.772	10.221
CoVSi	4.44	193.97	270.85	4.42
CoVGe	6.30	176.87	283.89	10.77

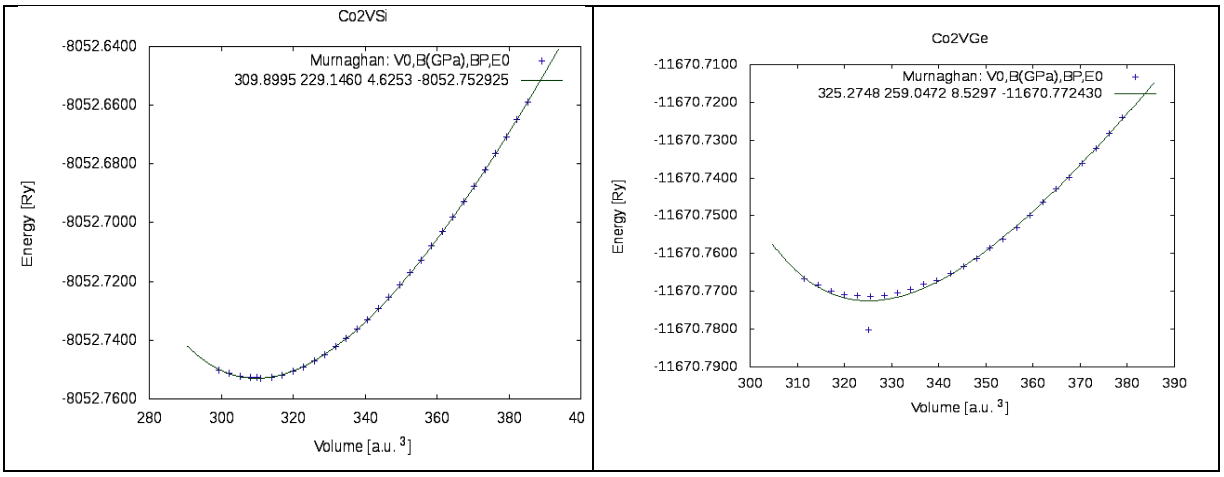

Fig. 1. Volume optimization for the lattice parameters (continued on next page)

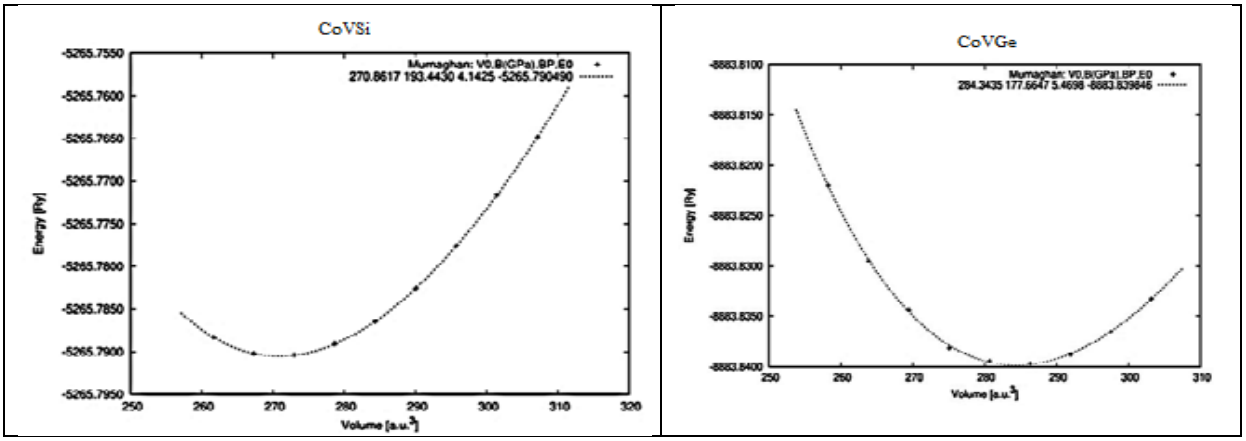

Fig. 1. *(continued)* Volume optimization for the lattice parameters

Electronic and magnetic properties:

The magnetic moment of a substance can change due to the spin of an electron. The band structure and density of state of the Heusler compound are used to study the change in magnetic moment. At the Fermi level, a compound is characterized as half metallic ferromagnetic if it exhibits metallic behavior in one spin channel and semiconducting or insulating behavior in the other spin channel. Spin polarization is the name given to these phenomena. Spintronics is a particularly intriguing topic of research in the modern day. The benefits of Spintronics devices include nonvolatile magnetic memory, magnetic sensors, tunnel junctions, higher data processing speed, increased integration intensities, and very fast data processing. These devices lower the amount of electricity consumed and the amount of heat dissipated. Spin polarized computations of Co2VZ (Z= Si, Ge) compounds were performed using the Generalized-gradient approximation (GGA) full Heusler at optimized lattice settings. The magnetic moment is caused by the intrinsic spin of the electron. Theoretical spin polarization values can be computed using the formula below.

$$P_n = \frac{n\uparrow - n\downarrow}{n\uparrow + n\downarrow}$$

If either $n_\uparrow = 0$ or $n_\downarrow = 0$, then $P_n = 1$ or -1. It indicates that if either up or down spin exists, spin polarization is 100%. These materials are referred to be half metals ferromagnetic [56]. If the P_n value is zero, the materials are paramagnetic or anti-ferromagnetic even below the magnetic transition temperature. The energy gap is the difference between the greatest energy occupied point in the valence band area and the lowest unoccupied energy point in the conduction band. The study of energy gap from DOS and band structure of the compounds Co2VZ (Z= Pb, Si, Sn) reveals that only Co_2VSi does not show a band gap in minority spin channel using WIEN2k code, indicating 100% spin polarization. When the code for the other two specified compounds (Co_2VPb and Co_2VSn) is run in WIEN2k, the band gaps are 0.33 and 0.54eV, indicating semiconducting behavior. The ATK-VNL code results demonstrate that all three compounds have a band gap in the down spin channel but no band gap in the up spin channel. Table 2 summarizes the obtained energy gap and spin polarization for the aforesaid entire Heusler compound. Figures 2-5 show the detailed results of band structures and density of states.

Table 2: Energy gap and spin polarization of Co_2VZ (Z= Si, Ge), CoVZ (Z= Si, Ge)

Compound	Energy gap E_g (eV)		Spin polarization
	Up spin	Down spin	
Co_2VSi	0.0	0.0	P_n vanishing
Co_2VGe	0.0	0.668	100%
CoVSi	0.663	0.680	P_n vanishing
CoVGe	0.688	0.701	P_n vanishing

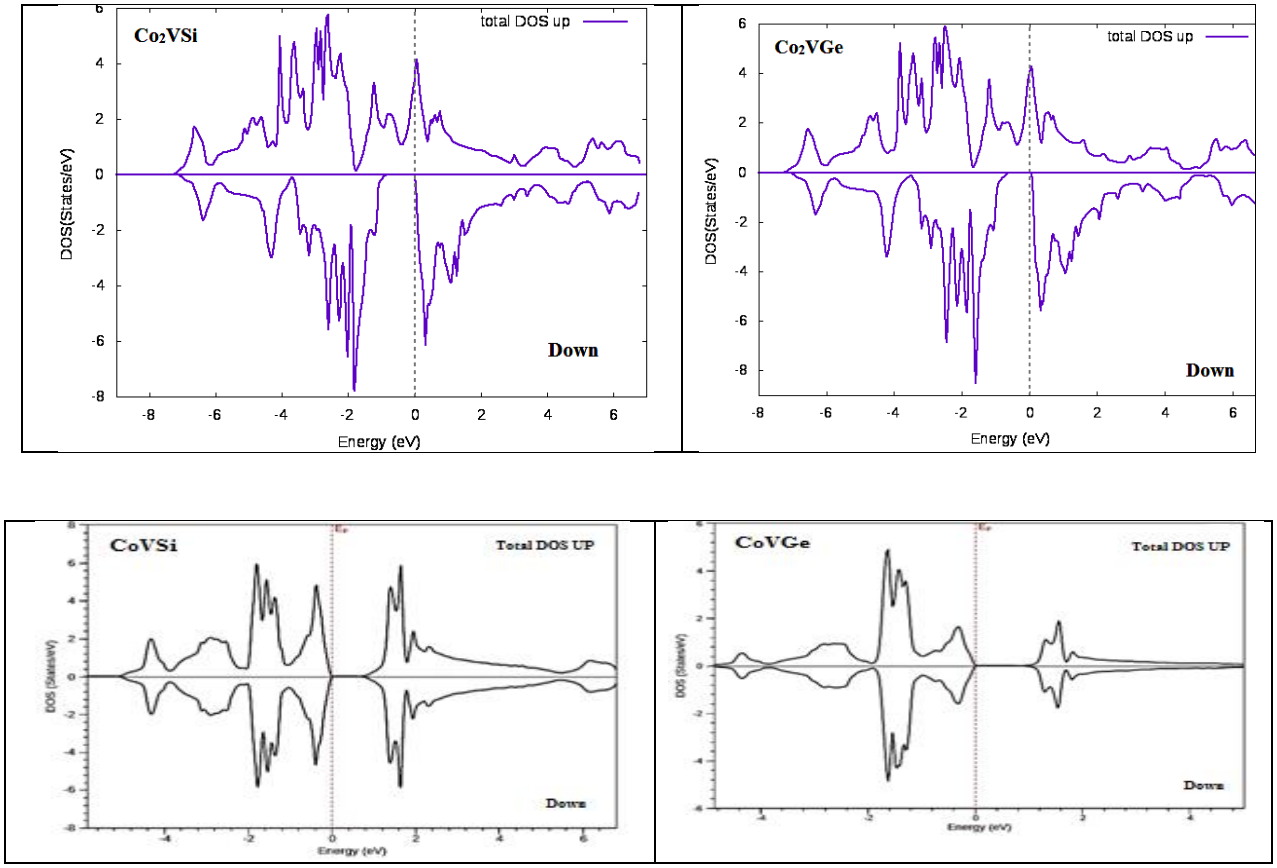

Fig. 3. DOS of Co_2VZ (Z= Si, Ge) and CoVZ (Z= Si, Ge)

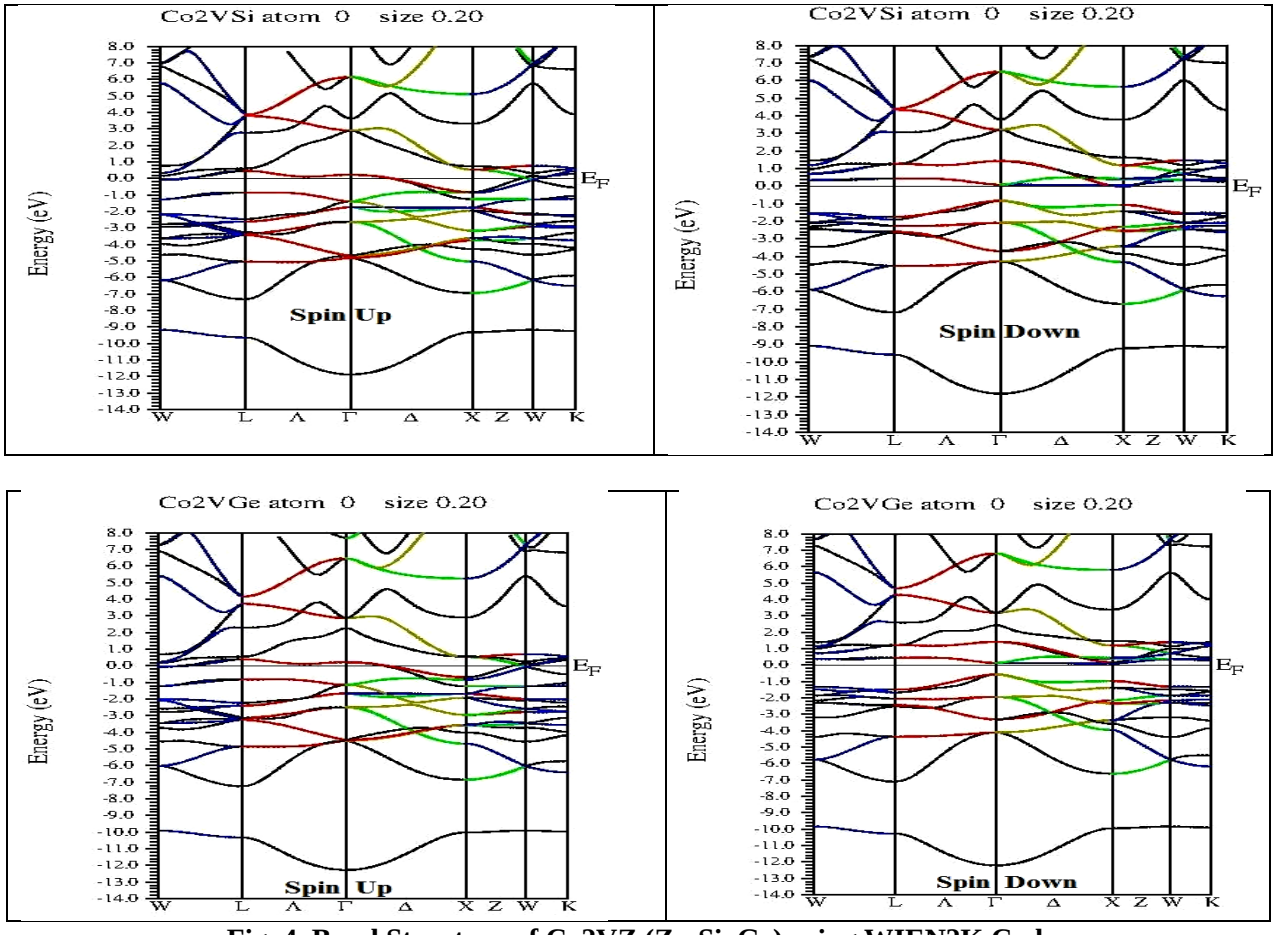

Fig. 4. Band Structure of Co2VZ (Z= Si, Ge) using WIEN2K Code

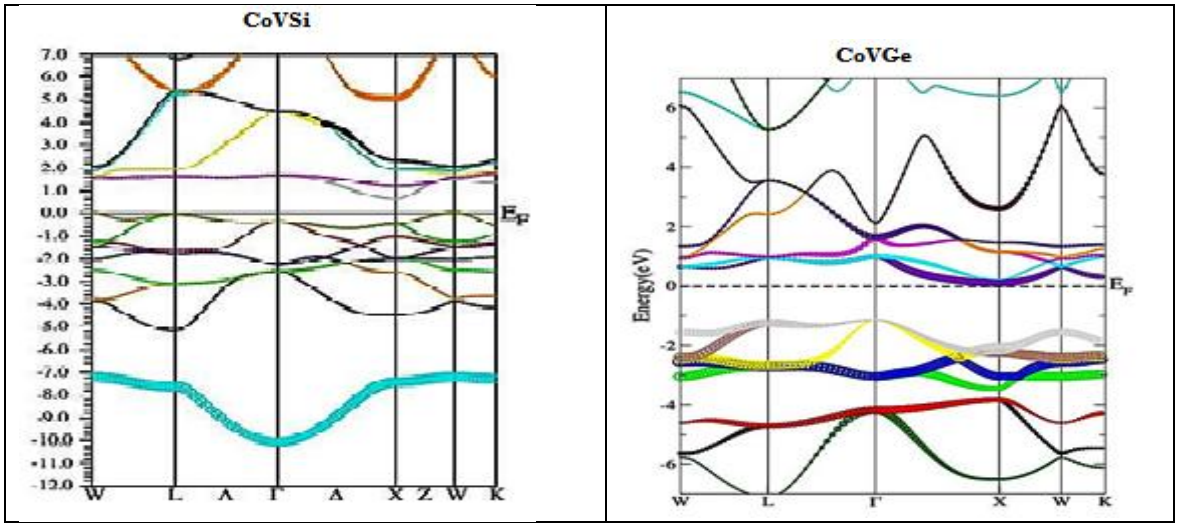

The number of valence electrons and the spin magnetic moment has a linear relationship. The fundamental clue of the Slater-Pauling rule is this simple relationship. J. C. Slater [57] and L. Pauling [58] derive a theoretical formula for estimating the magnetic moment per unit cell, which is known as the Slater-Pauling rule. According to this rule, if the total number of valence electrons in a full Heusler compound is equal to 24, the compound has zero magnetic moment; otherwise, the difference between the total number of valence electrons and 24 represents the net amount of spin magnetic moment per unit cell. Slater-Pauling developed this theoretical method for predicting magnetic moments. Method for Full Heusler compound is given as-

$M_t = Z_t - 24$

Where Mt is the total magnetic moment per unit cell and Z_t is the total valence electron count. Curie temperature and spin magnetic moment have a straightforward relationship in full Heusler compounds, i.e. Curie temperature is directly proportional to spin magnetic moment. After 24 hours, the Curie temperature of the ferromagnetic half-metallic Heusler compounds rises by 175 K per additional electron. The results of the codes WIEN2k and ATK-VNL are contrasted with those of the theoretical technique Slater-Pauling rule. Table 3 is particularly useful for analyzing magnetic moment values from WIEN2k, ATK-VNL code, and Slater-Pauling rule. The total number of valence electrons for all three Co_2CrZ compounds (Z= In, Sb, Sn) is 27. As a result of the Slater-Pauling rule, the magnetic moments per unit cell for all three compounds are 3.0 B. WIEN2k and ATK-VNL now produce values of 3.00 and 3.00, 3.02 and 2.96, 3.00 and 3.00, respectively. Except for a tiny change in the values of Co_2VSi, these compiled values are identical to the values of the theoretical technique Slater-Pauling. As a result, the listed compounds show good agreement with Slater-Pauling behavior. The investigation of the results reveals that the Co and Cr position atoms give the majority of the magnetic moment, with the Z position atom contributing a little portion. Table 3 summarizes the calculated results for magnetic moments for Co_2VZ (Z= Pb, Si, Sn) obtained using the full potential linearized augmented plane wave (FP-LAPW) method implemented in WIEN2k and the pseudo-potentials method implemented in Atomistic Tool Kit-Virtual NanoLab (ATK-VNL) within the Generalized-gradient approximation (GGA) for exchange correlation functions.

Table 4.Total magnetic moments of the compounds Co_2VZ (Z= Si, Ge), CoVZ (Z= Si, Ge)

Compound	Z_t	WIEN2k	Slater-Pauling (Z_t - 24) for Full Heusler & (Z_t - 18) for Half Heusler
Co2VSi	27	3.04	3.00
Co_2VGe	27	3.01	3.00
CoVSi	18	0.0	0.0
CoVGe	18	0.0	0.0

Elastic properties:

Elastic characteristics are the most basic qualities of a material that may be computed using the first principle method. Out of six independent constants, three reduced elastic constants C11, C12, and C44 govern cubic crystal elasticity. These three reduced elastic constants provide vital information on structure stability, mechanical characteristics, bond indices, and material anisotropy. The classical mechanical stability criteria of elastic constant must be met by the crystal. The following is the typical mechanical stability criterion for cubic crystal.

$C_{11} - C_{12} > 0$, $C_{11} > 0$, $C_{11} + 2C_{12} > 0$, $C_{44} > 0$, $C_{12} < B < C_{11}$ [59-60]

Anisotropic factor 'A' is used to calculate structural stability. If the value of 'A' equals one, the material is isotropic; if it deviates from one, the material is anisotropic. Isotropic material properties are those that do not change with orientation.

$$A = \frac{2C_{44}}{C_{11} - C_{12}}$$

Bond index, given as CP = C_{12} - C_{44}, can be used to determine a material's stiffness and flexibility. If the value is positive, the substance is metallic in nature; if the value is negative, the material is nonmetallic. Furthermore, a positive result indicates that the material is ductile, while a negative result indicates that the material is brittle. If the bond index value is less than 12, it indicates soft material, and if it is larger than 12, it indicates hard material [61]. Pugh's B/G ratio is also used to determine if a material is brittle or ductile. If the B/G ratio is less than 1.75, the material is brittle; if the B/G ratio is larger than 1.75, the material is ductile. The mechanical characteristics of the compounds are obtained by the Voigt-Reuss-Hill (VRH) averaging method using the Bulk modulus (B), Young modulus (E), Shear modulus (G), and Poisson ratio (v). Formulas for B, E, G, and v using the elastic constant are as follows:

$$B = B_V = B_R = \frac{C_{11} + 2C_{12}}{3} G = \frac{G_V + G_R}{2}$$

$$G_V = \frac{C_{11} - C_{12} + 3C_{44}}{5} G_R = \frac{5C_{44}(C_{11} - C_{12})}{[4C_{44} + 3(C_{11} - C_{12})]}$$

(V = Voigt and R = Reuss)

Young modulus is also used to calculate material stiffness. This is possible in terms of B and G.

$$E = \frac{9BG}{3B + G}$$

In terms of B and G, the Poisson ratio can be determined. For the most part, the Poisson ratio is between 0 and 0.5.

$$v = \frac{3B - 2G}{2(3B + G)}$$

The Atomistic Tool Kit-Virtual NanoLab (ATK-VNL) programme is used here, with the Pseudo-potential approach applied in the framework of density functional theory (DFT). Table 4 compiles all of the findings obtained from this code.

Table 4: Elastic constants and bulk moduli B (GPa), shear moduli G (GPa), Young's modulus E (GPa), B/G values, Poisson's ratio v, and anisotropy factor A of Co2VZ (Z= Si, Ge) compounds.

Compound	Elastic constant			B (GPa)	G (GPa)	E (GPa)	B/G	*v*	A
	C_{11}	C_{12}	C_{44}						
Co_2VSi	272.09	215.87	138.02	234.61	73.94	200.74	3.17	0.36	4.91
Co_2VGe	229.03	209.81	117.04	216.21	47.73	133.37	4.53	0.40	12.18
CoVSi	294.20	134.60	89.20	187.80	85.31	222.28	2.20	0.30	1.12
CoVGe	294.40	114.10	119.70	174.20	106.85	266.14	1.63	0.25	1.33

Table 4 shows that the classic mechanical stability criterion C11 - C12 > 0, C11 > 0, C11 + 2C12 > 0, C44 > 0, C12 B C11 is satisfied for all the compounds Co2VZ (Z= Pb, Si, Sn). For all three compounds, the anisotropic constant 'A' deviates from one. As a result, we conclude that the compounds Co2VZ (Z= Pb, Si, Sn) are anisotropic. Poisson values range from zero to 0.5. Table 5 reveals that the Pugh's ratio B/G for all chemicals in the table is more than 1.75. As a result, the materials mentioned above are ductile in nature. Cauchy pressure (CP = C12 - C44) values collected from table 5 are positive for these compounds Co2VZ (Z= Pb, Si, Sn) and indicate metallic character.

CONCLUSIONS:

The first principle technique was used to investigate the structural, electrical, optical, and magnetic properties of Co_2VZ (Z= Pb, Si, Sn) compounds. We use two separate codes to create the findings for the above attributes of the listed substances. The first is the full potential linearized augmented plane wave (FP-LAPW) method implemented in WIEN2k, and the second is the pseudo-potentials method implemented in Atomistic Tool Kit-Virtual NanoLab (ATK-VNL) within the Generalized-gradient approximation (GGA) for exchange and correlation function. According to the results of this investigation, two of the three compounds exhibit half metallicity and

100% spin polarization with L21 ordered stable structures, with the exception of Co2VSi in the full potential linearized augmented plane wave (FP-LAPW) approach. The pseudo-potentials technique, on the other hand, reveals that all three compounds have half metallicity and 100% spin polarization with L21 ordered stable structures. Magnetic moments calculated per unit cell agree well with Slater-Pauling behavior. The reflectivity, refractive index, excitation coefficient, absorption coefficient, optical conductivity, and electron energy loss spectra of these compounds were studied. As the value of energy grows, so do the values of the absorption coefficient and the electron energy-loss function. According to the projected results, the compounds Co2VZ (Z= Pb, Sn) are suitable for Spintronics applications. The elastic characteristics of the above-mentioned combinations indicate that they are ductile and metallic in nature.

REFERENCES:

1. M.M. Obeid, H.R. Jappor, S.J. Edrees, M.M. Shukur, R. Khenata, Y. Mogulkoc, The electronic, half-metallic, and magnetic properties of Ca1-xCrxS ternary alloys: insights from the first-principle calculations, J. Mol. Graph. Model. 89 (2019) 22–32.
2. U. Rani, Y. Soni, P.K. Kamlesh, A. Shukla, A.S. Verma, Fundamental theoretical design of Na-ion and K-ion based double antiperovskite X6SOA2 (X Na, K; A Cl, Br and I) halides: potential candidate for energy storage and harvester, Int. J. Energy Res. 45 (2021) 13442–13460.
3. U. Rani, P.K. Kamlesh, R. Agarwal, J. Kumari, A.S. Verma, Electronic and thermo- physical properties of double antiperovskites X6SOA2 (X Na, K and A Cl, Br, I): a non-toxic and efficient energy storage materials, Int. J. Quant. Chem. (2021) 26759.
4. M.M. Obeid, M.M. Shukur, S.J. Edrees, R. Khenata, M.A. Ghebouli, S.A. Khandy, A. Bouhemadou, H.R. Jappor, X. Wang, Electronic band structure, thermodynamics and optical characteristics of BeO1 xAx (A S, Se, Te) alloys: insights from ab initio study, Chem. Phys. 526 (2019) 110414.
5. G.J. Snyder, E.S. Toberer, Complex theramoelectric materials, in: Materials for Sustainable Energy: A Collection of Peer-Reviewed Research and Review Articles from Nature Publishing Group, World Scientific Publishing Co., 2010, pp. 101–110.
6. I.S. Khare, N.J. Szymanski, D. Gall, R.E. Irving, Electronic, optical, and thermoelectric properties of sodium pnictogen chalcogenides: a first principles study, Comput. Mater. Sci. 183 (2020) 109818.
7. S. Choudhary, A. Shukla, J. Chaudhary, A.S. Verma, Extensive investigation of structural, electronic, optical, and thermoelectric properties of hybrid perovskite (CH3NH3PbBr3) with mechanical stability constants, Int. J. Energy Res. 44 (2020) 11614–11628.
8. M.I. Hussain, R.M.A. Khalil, F. Hussain, A.M. Rana, DFT -based insight into the magnetic and thermoelectric characteristics of XTaO3 (X Rb, Fr) ternary perovskite oxides for optoelectronic applications, Int. J. Energy Res. 45 (2020) 2753–2765.
9. M. Lindorf, K. Mazzio, J. Pflaum, K. Nielsch, W. Brütting, M. Albrecht, Organic- based thermoelectrics, J. Mater. Chem. A 8 (2020) 7495–7507.
10. J. Chu, J. Huang, R. Liu, J. Liao, X. Xia, Q. Zhang, C. Wang, M. Gu, S. Bai, X. Shi, L. Chen, Electrode interface optimization advances conversion efficiency and stability of thermoelectric devices, Nat. Commun. 11 (2020) 2723.
11. S.P. Singh, N. Kanas, T.D. Desissa, M. Johnsson, M.-A. Einarsrud, T. Norby, K. Wiik, Thermoelectric properties of A-site deficient La-doped SrTiO3 at 100-900 ◦C under reducing conditions, J. Eur. Ceram. Soc. 40 (2019) 401–407.
12. P.K. Kamlesh, R. Gautam, S. Kumari, A.S. Verma, Investigation of inherent properties of XScZ (X = Li, Na, K; Z = C, Si, Ge) half-Heusler compounds: appropriate for photovoltaic and thermoelectric applications, Phys. B Condens. Matter 615 (2021) 412536.
13. U. Chopra, M. Zeeshan, S. Shambhawi, R. Dhawan, H.K. Singh, J. van den Brink, H.C. Kandpal, First–principles study of thermoelectric properties of Li–based Nowotony–Juza phases, J. Phys. Condens. Matter 31 (2019) 505504.
14. S.A. Sofi, D.C. Gupta, Systematic study of ferromagnetic phase stability of Co- based Heusler materials with high figure of merit: hunt for spintronics and thermoelectric applicability, AIP Adv. 10 (2020) 105330.
15. S.S. Shastri, S.K. Pandey, First-principles electronic structure, phonon properties, lattice thermal conductivity and prediction of figure of merit of FeVSb half- Heusler, J. Phys. Condens. Matter, (2020), 085714.
16. A. Mukhopadhyay, N. Lakshminarasimhan, N. Mohapatra, Electronic, thermal and magneto-transport properties of the half-Heusler, DyPdBi, Intermetallics 110 (2019) 106473.

17. M. Hammou, F. Bendahma, M. Mana, S. Terkhi, N. Benderdouche, Z. Aziz B. Bouhafs, Thermoelectric and half-metallic behavior of the novel Heusler alloy RbCrC: ab- initio DFT study, Spin 10 (2020) 2050029, https://doi.org/10.1142/ S2010324720500290.
18. A. Roy, J.W. Bennett, K.M. Rabe, D. Vanderbilt, Half-heusler semiconductors as piezoelectrics, Phys. Rev. Lett. 109 (2012), 037602.
19. A. Hussain, M. kashif, M. Belabbas, M. Noreen, F. ur R. Janjua, O. Arbouche, First principle calculation of mechanical stability, opto-electronic and thermo-electric properties of TaIrGeSn (0 x 1) Half-Heusler alloy, Computational Condensed Matter 25 (2020), e00511.
20. S. Chadov, X. Qi, J. Kübler, G.H. Fecher, C. Felser, S.C. Zhang, Tunable multifunctional topological insulators in ternary Heusler compounds, Nat. Mater. 9 (2010) 541–545.
21. A.S. Sukhanov, Y.A. Onykiienko, R. Bewley, C. Shekhar, C. Felser, D.S. Inosov, Magnon spectrum of the Weyl semimetal half-Heusler compound GdPtBi, Phys. Rev. B 101 (8) (2020), 014417.
22. R.F. Wang, S. Li, W.-H. Xue, C. Chen, Y.-M. Wang, X.-J. Liu, Q. Zhang, Enhanced thermoelectric performance of n-type TiCoSb half-Heusler by Ta doping and Hf alloying, Rare Met. 40 (2020) 40–47.
23. H.R. Jappor, Z.A. Saleh, M.A. Abdulsattar, Simulation of electronic structure of aluminum phosphide nanocrystals using ab initio large unit cell method, Advances in Materials Science and Engineering 2012 (2012) 180679.
24. D. Shrivastava, S.P. Sanyal, Theoretical study of structural, electr0nic, phonon and thermoelectric properties of KScX (X Sn and Pb) and KYX (X Si and Ge) half-Heusler compounds with 8 valence electrons count, J. Alloys Compd. 784 (2019) 319–329
25. R. Ahmad, N. Mehmood, A density functional theory investigations of half- heusler compounds RhVZ (Z P, as, Sb), J. Supercond. Nov. Magnetism 31 (2017) 1577–1586.
26. S. Ju, J. Shiomi, Materials informatics for heat transfer: recent progresses and perspectives, Nanoscale Microscale Thermophys. Eng. 23 (2019) 157–172.
27. A. Afaq, M. Rizwan, A. Bakar, Computational investigations of XMgGa (X Li, Na) half Heusler compounds for thermo-elastic and vibrational properties, Phys. B Condens. Matter 554 (2018) 102–106.
28. A. Besbes, R. Djelti, B. Bestani, Optical and thermoelectric response of RhTiSb half-Heusler, Int. J. Mod. Phys. B 33 (2019) 1950247.
29. B. Vikram, C.K. Sahni, Barman, A. Alam, Accelerated discovery of new 8-electron half-heusler compounds as promising energy and topological quantum materials, J. Phys. Chem. C 123 (2019)7074–7080
30. S.H. Shah, S.H. Khan, A. Laref, G. Murtaza, Optoelectronic and transport properties of LiBZ (B Al, In, Ga and Z Si, Ge, Sn) semiconductors, J. Solid State Chem. 258 (2018) 800–808. F. Heusler, Über magnetischemanganlegierungen, Verhandlungen Dtsch. Phys. Ges. 5 (1903) 219.
31. Ohnuma, M. Matsuo, S. Maekawa, Spin transport in half-metallic ferromagnets. Phys. Rev. B. 94 (2016) 184405.
32. S. M. Griffin, J. B. Neaton, Prediction of a new class of half-metallic ferromagnets from first principles. Phys. Rev. Mater. 1 (2017) 044401.
33. N. I. Kourov, V. V. Marchenkov, K. A. Belozerova, H. W. Weber, Specific features of the electrical resistivity of half- metallic ferromagnets Fe2MeAl (Me = Ti, V, Cr, Mn, Fe, Ni). J. Exper. Theor. Phys. 118 (2014) 426-431.
34. M. Sun, Q. Ren, Y. Zhao, S. Wang, J. Yu, W. Tang, Magnetism in transition metal-subsititued germanane: A search for room temperature spintronic devices, J. Appl. Phys. 119 (2016) 143904.
35. I. Galanakis, K. Özdoğ an, E. Ş aşioğ lu, Spin-filter and spin-gapless semiconductors: The case of Heusler compounds, AIP Adv. 6 (2016) 055606
36. Y. Wang, R. Ramaswamy, H. Yang, FMR-related phenomena in spintronic devices, J. Phys. D. Appl. Phys. 51 (2018) 273002.
37. Y. Feng, Z. Cui, M. S. Wei, B. Wu, Spin-polarized quantum transport in Fe4N based current-perpendicular-to-plane spin valve. App. Surf. Sci.499 (2019) 78–83.
38. R.A. De Groot, F.M. Muller, P. G.Van Engen and K.H.J. Buschow, New class of materials: half- metallic ferrowmagnets, Phys. Rev. Lett. 50 (1983) 2024-2027.
39. A. Aguayo, G. Murrieta, Density functional study on the half-metallic ferromagnetism in Co-based Heusler alloys Co2MSn (M=Ti, Zr, Hf) using LSDA and GGA, Journal of Magnetism and Magnetic Materials, 323 (2011) 3013-3017.
40. Sukhender, Lalit Mohan, Sudesh Kumar,

Deepak Sharma, Ajay Singh Verma, Structural, electronic, optical and magnetic properties of Co_2CrZ (Z= Al, Bi, Ge, Si) Heusler compounds, East Eur. J. Phys. **2** (2020) 69-80. https://doi.org/10.26565/2312-4334-2020-2-05

41. Sukhender, Pravesh Pravesh, Lalit Mohan, Ajay Singh Verma, Ductile and metallic nature of Co_2VZ (Z= Pb, Si, Sn) Heusler compounds: a first principles study, East Eur. J. Phys., **3** (2020) 99-110. https://doi.org/10.26565/2312-4334-2020-3-13
42. Sukhender**,** Pravesh Pravesh, Lalit Mohan, Ajay Singh Verma, First principles calculations for electronic, optical and magnetic properties of full heusler compounds, East Eur. J. Phys. **3** (2020) 111-121. https://doi.org/10.26565/2312-4334-2020-3-14
43. Sukhender, Lalit Mohan, Ajay Singh Verma, Electronic, optical, elastic and magnetic properties of Co_2VZ (Z= As, B, In, Sb) Heusler compounds, East Eur. J. Phys., **4** (2020) 51-62. https://doi.org/10.26565/2312-4334-2020-4-07
44. F. Gregor, K. Perter, Ternary semiconductors NiZrSn and CoZrBi with half- Heusler structure: A first-principles study. Phys. Rev. B. 94 (2016) 075203.
45. C. K. Barman, A. Alam, Topological phase transition in the ternary half-Heusler alloy ZrIrBi. Phys. Rev. B. 97 (2018) 075302.
46. S. Ishida, S. Akazawa, Y. Kubo, J. Ishida, Band theory of Co_2MnSn, Co_2TiSn and Co_2TiAl, J. Phys. F: Met. Phys. 12 (1982) 1111.
47. J. Kübler, A.R. William, C.B. Sommers, Formation and coupling of magnetic moments in Heusler alloys. Phys. Rev. B 28 (1983) 1745-1755.
48. Y. Miura, K. Nagao and M. Shirai, Atomic disorder effects on half-metallicity of the full-Heusler alloys Co2(Cr1−xFex)Al: A first-principles study, Phys. Rev. B 69 (2004) 144413.
49. J. Kübler, G. H. Fecher, C. Felser, Understanding the trend in the Curie temperatures of Co_2- based Heusler compounds: Ab initio calculations. Phys. Rev. B 76 (2007) 024414
50. S. A. Wolf, D. D. Awschalom, R. A. Buhrman, J. M. Daughton, S. V. Molnar, M. L. Roukes, A. Y. Chtchelkanova, D. M. Treger, Spintronics: a spin-based electronics vision for the future, Science, 294 (2001) 1488-1495.
51. E. Şaşıoğlu, L. M. Sandratskii, P. Bruno, I. Galanakis, Exchange Interactions and Temperature Dependence of Magnetization in half-Metallic Heusler Alloys, Phys. Rev. B., 72 (2005) 184415.
52. S. Wurmehl, G. H. Fechel, H. C. Kandpal, V. Ksenofontov, C. Felser, H. Lin, Investigation of Co2FeSi: The Heusler compound with highest Curie temperature and magnetic moment, Appl. Phys. Lett., 88 (2006) 032503.
53. I. Galanakis, Surface Properties of the Half and full-Heusler Alloys, J. Phys.: Condens. Matter, 14 (2002) 6329-6340.
54. I. Galanakis, P. H. Dederichs, N. Papanikolaou, Origin and properties of the gap in the half-ferromagnetic Heusler alloys. Phys. Rev. B 66 (2002) 134428
55. T. Block, C. Felser, G. Jakob, J. Ensling, B. Muhling, P. Gutlich, V. Beaumont, F. Studer and R. J. Cava, Large negative magnetoresistance effects in $Co_2Cr_{0.6}Fe_{0.4}Al$, J. Solid Solid State Chem., 176 (2003) 646-651.
56. E. Wimmer, H. Krakauer, M. Weinert, and A. J. Freeman, Full-potential self-consistent linearized-augmented-plane-wave method for calculating the electronic structure of molecules and surfaces: O2 molecule, Phys. Rev. B 24 (1981) 864-875.
57. P. Blaha, K. Schwarz, G. K. H. Madsen, D. Kvasnicka and J. Luitz in WIEN2k, An Augmented Plane Wave + Local Orbitals Program for Calculating Crystal Properties, edited by K Schwarz (Technical Universitatwien, Austria, (2001), ISBN 3-9501031-1-2.
58. J. P. Perdew, K. Burke and M. Ernzerhof, Generalized gradient approximation made simple, Phys. Rev. Lett. 77 (1996) 3865-3868.
59. J. P. Perdew, K. Burke, Y. Wang, Generalized gradient approximation for the exchange-correlation hole of a many-electron system, Phys. Rev. B. 54 (1996) 16533
60. E. Sjostedt, L. Nordstrom and D. J Singh, An alternative way of linearizing the augmented plane- wave method, Solid State commun. 114 (2000) 15-20.
61. Atomistix ToolKit-Virtual Nanolab (ATK-VNL), QuantumWise Simulator, Version. 2014.3.[Online]. Available: http://quantumwise.com/
62. Y. J. Lee, M. Brandbyge, J. Puska, J. Taylor, K. Stokbro and M. Nieminen, Electron transport through monovalent atomic wises, Phys. Rev. B, 69 (2004) 125409.
63. K. Schwarz DFTcalculations of solids with LAPW and WIEN2k J. Solid State Chem. 176 (2003) 319–328.
64. P. Pulay, ImprovedSCF convergence acceleration. J. Comput. Chem. 3 (1982) 556–560.
65. H. J. Monkhorst, and J. D. Pack, Special points for Brillouin-zone integrations, Phys. Rev. B

13 (1976) 5188-5192.
66. P. J. Webster, Magnetic and chemical order in Heusler alloys containing cobalt and manganese, J. Phys. Chem. Sol. 32 (1971) 1221-1231.
67. Fr. Heusler, Ueber magnetische Manganlegierungen. Verh. Dtsch. Phys. Ges. 5(1903) 219.
68. F. D. Murnaghan, The compressibility of media under extreme pressures, Proc. Natl. Acad. Sci. U. S. A. 30 (1944) 244-247.
69. Jr. R. J. Soulen, J. M. Byers, M. S. Osofsky, B. Nadgorny, T. Ambrose, S. F. Cheng, P. R. Broussard, C. T. Tanaka, J. Nowak, J. S. Moodera, A. Barry and J. M. D. Coey, Measuring the Spin Polarization of a Metal with a Superconducting Point Contact. science 282 (1998), 85-88.
70. J. C. Slater, The Ferromagnetism of Nickel, Phys. Rev. 49 (1936) 537-545.
71. L. Pauling, The Nature of the Interatomic Forces in Metals, Phys. Rev. 54 (1938) 899-904.
72. Y. V. Kudryavtsev, N. V. Uvarov, V. N. Iermolenko and J. Dubowik, Electronic structure, optical, and magneto-optical properties of Co 2 CrGa Heusler alloy films: Experimental and theoretical study, J. Appl. Phys. 108 (2010) 113708.
73. N. V. Uvarov, Y. V. Kudryavtsev, A. F. Kravets, A. Ya. Vovk, R. P. Borges, M. Godinho, and V. Korenivski, Electronic structure, optical and magnetic properties of Co2FeGe Heusleralloy films, J. Appl. Phys. 112 (2012) 063909.
74. M. Born, K. Huang, Dynamical Theory of Crystal Lattices, Clarendon, Oxford 1956, p. 420.
75. A. Akriche, H. Bouafia, S. Hiadsi, B. Abidri, B. Sahli, M. Elchikh, M.A. Timaoui, B. Djebour First-principles study of mechanical, exchange interactions and the robustness in Co2MnSi full Heusler compounds, Journal of Magnetism and Magnetic Materials. 422 (2017) 13-19.
76. D. G. Pettiifor, Theoretical predictions of structure and related properties of intermetallics, J. Mater. Sci. Technol. 8 (1992) 345-349.
77. R. Hill, The elastic behaviour of a crystalline aggregate, Proc. Phys. Soc., A 65 (1952) 349-354.
78. A.Hamidani, B. Bennecer, B. Boutarfa,Structural and elastic Properties of the full-Heusler compounds IrMnZ (Z = Sn, Al and Sb), Materials Chemistry and Physics. 114 (2009) 732-735.